Identification and structural characterization of biodegradation products of atenolol and glibenclamide by liquid chromatography coupled to hybrid quadrupole time-of-flight and quadrupole ion trap mass spectrometry

J. Radjenović[a], S. Pérez[a], M. Petrović[a,b], D. Barceló[a,c,*]

[a] Department of Environmental Chemistry, IDAEA-CSIC, c/Jordi Girona 18-26, 08034 Barcelona, Spain
[b] Institucio Catalana de Recerca i Estudis Avançats (ICREA), Barcelona, Spain
[c] Catalan Institute for Water Research (ICRA), Parc Científic I Tecnológic de la Universitat de Girona, Edifici Jaume Casademont, Porta A, Planta 1-Despatx 13C/Pic de Peguera, 15, E-17003 Girona, Spain

ARTICLE INFO

ABSTRACT

In this paper we report about the biodegradation of the β-blocker atenolol and the hypoglycaemic agent glibenclamide. The biodegradation tests were performed in batch reactors under aerobic conditions, using as inocculums sewage sludge from a conventional activated sludge treatment and a laboratory-scale membrane bioreactor. Pharmaceuticals were used as sole carbon sources, spiked at 50 ng/L and 10 mg/L concentrations. Quadrupole time-of-flight mass spectrometry coupled to ultra-high-pressure liquid chromatograph was used for the screening and the structural elucidation of biodegradation products. A microbial metabolite of atenolol with $[M+H]^+$ at 268 was detected in the positive electrospray ionization mode. This new compound was determined to be a product of microbial hydrolysis of the amide of the parent compound. Biodegradation of glibenclamide by activated sludge proceeded via bacterial hydroxylation of the cyclohexyl ring, which resulted in formation of metabolite with a protonated molecule, $[M+H]^+ = 510$. MS^3 experiments performed by hybrid quadrupole linear ion trap (QqLIT) mass spectrometry coupled to high-performance liquid chromatography enabled further structural elucidation of the identified metabolites. Moreover, the highly sensitive QqLIT instrument in the MRM mode enabled the detection of parent compounds and one of the microbial metabolites identified in real wastewater samples. The methodology used in this study permitted for the first time the identification and detection of biodegradation product of β-blocker atenolol in real wastewater samples.

© 2008 Elsevier B.V. All rights reserved.

1. Introduction

Little is known about the extent of environmental occurrence and ultimate fate of pharmaceutical residues. Their continuous input into the environment maintains their concentrations relatively constant, even for the non-persistent drugs. This raises many questions on the effect that pharmaceutically active compounds (PhACs) might have on the aquatic life and potentially humans, through drinking water supplies. Information on the potential adverse health effect of drugs in aqueous environmental media is still lacking [1]. Furthermore, products of their photolytic and microbial degradation may be more persistent and have their own biological activity that can contribute to the overall toxicity. With these facts in view, transformation and degradation products of pharmaceuticals need to be considered as well

for a comprehensive study of the behaviour and ecotoxicity of drugs in the environment. The studies on the identification of biodegradation products of pharmaceuticals are still very scarce [2–5]. Zwiener et al. [2] performed batch experiments with activated sludge and identified hydroxyibuprofen as a major metabolite of oxic degradation of the anti-inflammatory drug ibuprofen. 4-Chlorobenzoic acid was found to be formed by hydrolytic cleavage of the amide bond from the lipid regulator bezafibrate, while ketoprofen was degraded as a sole substrate along the pathway known for biphenyls and related compounds [4]. Similar to bezafibrate and ibuprofen, another anti-inflammatory drug naproxen was also degraded co-metabolically leading to the formation of desmethylnaproxen as the initial step of mineralization [4]. Nitrifying activated sludge bacteria were found to oxidize the antibiotic trimethoprim to α-hydroxytrimethoprim [3], whereas this drug was reported to be persistent during the activated sludge treatment [6]. For the X-ray contrast agent iopromide different metabolites were reported for aerobic degradation by nitrifying and activated sludge [5].

Since one of the main routes for human pharmaceuticals to enter the environment is via treated wastewater effluents, their elimination during the treatment is crucial for the assessment of environmental impact of a wastewater treatment plant (WWTP). In recent years the use of membrane bioreactor (MBR) technology for the treatment of wastewater has gained a lot of attention. Besides obvious advantages of this type of treatment compared to the conventional activated sludge (CAS) process (e.g. enhanced biological performance, complete retention of solids, and smaller footprint), MBR seems to be an efficient barrier for the passage of micropollutants [7]. Several investigations on the performance of MBR have proved it to be very efficient in removing various therapeutic classes of pharmaceuticals [8–12]. This can be assumed to be due to the prolonged solids retention time (SRT) of MBR sludge compared to that of the conventional one, where specialized microorganisms have more time to proliferate and adapt to the present trace organics.

In this paper the attention is focused on biotransformation/biodegradation routes of the β-blocker atenolol and the hypoglycemic agent glibenclamide. Atenolol is one of the most commonly prescribed cardioselective β-adrenergic blockers, used in antihypertensive, antianginal and antiarrhythmic treatment. After human consumption, it is excreted via urine mainly as an unchanged compound (90%) [13], with a small percentage of atenolol–glucuronide (0.8–4.4%) and hydroxyatenolol (1.1–4.4%, hydroxylation of the benzilic position) [14]. Glibenclamide, also known as glyburide, is an anti-diabetic drug, used in the treatment of type II diabetes. It is extensively metabolized, mainly by hydroxylation of the cyclohexyl moiety of the molecule, whereas its excretion rate as a parent compound are rather low, 35% and 42% in urine and faeces, respectively [15]. Both drugs were frequently detected in WWTP influents at ng/L concentration level, whereas in some cases comparable concentrations in the treated effluent were noticed [8,16–22]. As far as their environmental hazardousness is considered, the toxicity of atenolol as individual compound was found to be negligible [23]. However, although specific environmental effect of atenolol is low, in a mixture with other β-blockers (e.g. metoprolol, propranolol) it can contribute to the effect of concentration addition, as shown in tests with *Daphnia magna* [23]. The synergistic effect of β-blockers was also shown in phototoxicity assays conducted by Escher et al. [14], based on the inhibition of photosynthesis efficiency in green algae.

As discussed above, if during wastewater treatment stable metabolites of microbial degradation of drugs are formed, they would have to be addressed as well in the risk assessment analysis of pharmaceutical residues. In order to study the biodegradation pathways of the above-mentioned pharmaceuticals and elucidate possible differences between these routes in the conventional and advanced wastewater treatment, batch experiments were performed with two types of sludge: one originating from a full-scale CAS treatment and other from a laboratory-scale MBR operating in parallel with CAS. For the screening and structural elucidation of possible metabolites, a quadrupole time-of-flight (QqTOF) instrument was employed. In order to gain more structural information a hybrid quadrupole linear ion trap (QqLIT) instrument with MS^3 capability was used, revealing characteristic fragmentation patterns of the investigated compounds and their unknown metabolites. This study reports the identification of yet unknown products of microbial degradation of atenolol and glibenclamide, using two different approaches employing QqTOF and QqLIT mass spectrometers. Furthermore, for the first time the presence of a microbial metabolite of atenolol was confirmed in real wastewater samples using QqLIT mass spectrometry.

2. Experimental

2.1. Chemical standards

Atenolol (CAS No. 29122-68-7) was purchased from Sigma–Aldrich (St. Louis, MO, USA). Glibenclamide was kindly supplied by Dr. Marijan Ahel (Center for Marine and Environmental Research, Ruđer Boškovicǐ Institute, Zagreb, Croatia). All organic solvents were Chromasol LC grade. Water was purchased from Sigma–Aldrich, and acetonitrile, formaldehyde and methanol were from Riedel-de Haen (Seelze, Germany). Formic acid (Suprapur, >98%) was obtained from Merck (Darmstadt, Germany).

2.2. Biodegradation and sorption experiments

The sludge used in biodegradation and sorption experiments was obtained from WWTP Rubí, situated 20 km from Barcelona, Spain. WWTP Rubí was designed for 125.550 equivalent inhabitants. The treatment consists of a pre-treatment, preliminary treatment, primary sedimentation unit and a secondary (biological) treatment. In the premises of WWTP Rubí a submerged MBR was installed, operating in parallel with the CAS treatment. MBR of approximately 21 L of active volume was equipped with two flat sheet membranes (A4 size, area 0.106 m^2, pore size 0.4 μm) purchased from Kubota (Osaka, Japan). The biocenosis of the laboratory-scale MBR was grown from the inoculated sludge taken from the aeration basin and cultivated over a period of approximately 3 months, with no sludge discharge.

Biodegradation experiments were conducted in 1 L amber glass bottles pre-rinsed with ultra-pure water. The first set of biodegradation experiments was performed with sludge taken from the aeration basin of CAS treatment (i.e., conventional sludge), which operated with SRT of approximately 3 days. Inocculums of 1 L of freshly collected sludge were amended with 50 ng/L and 10 mg/L concentrations of each pharmaceutical as a sole substrate. The purpose of this was to identify any possible metabolites using mass spectrometric identification, with the initial 10 mg/L concentration of a parent compound. Also, the lower test concentration of 50 ng/L was used to investigate if the biodegradation pattern determined at 10 mg/L would repeat at environmentally relevant concentration levels. In the second part of experiments, biodegradation assays were performed with sludge originating from a laboratory-scale MBR operating at WWTP Rubí. 1 L volumes of MBR sludge were spiked at 10 mg/L concentrations of each compound. The suspended solids (SS) concentration of sludge proceeding from CAS treatment was approximately 4 g/L, whereas the SS concentration of MBR sludge was around 20 g/L. The pH value of both inoculations was in the range of pH 5.1–6.3.

The sludge volumes were maintained in all biodegradation trials performed by adding water (HPLC grade). The bottles with sludge inocculums were aerated through PTFE tubing continuously during 26 days, which was also preventing deposition of particulate matter. Samples were collected daily (1 mL) with the addition of 50 μL of formaldehyde to each sample, and they were frozen to −20 °C for preservation until the analysis. The analysis was done by ultra-high-pressure liquid chromatography (UHPLC)/positive electrospray ionization [(+)-ESI] QqTOF-MS monitoring a mass range from *m/z* 50 to *m/z* 800, and by HPLC/(+)-ESI-QqLIT-MS.

For the sorption experiments, test flasks with 1 L of autoclaved sewage sludge proceeding from the aeration basin at WWTP Rubí were spiked at 10 mg/L concentration of each pharmaceutical. The sludge was sterilized at P Selecta autoclave (Eleco-Remer, Uruguay) under 2 bar pressure and 121 °C temperature during 20 min. The flasks were continuously shaken with a magnetic stirrer and turbulence in the test solution kept the sludge particles of from settling.

Samples were collected in the first 1 h, 2 h, 5 h and 8 h, and afterwards daily during 10 days.

2.3. UHPLC/ESI-QqTOF-MS analysis

Accurate mass MS and MS/MS analyses of parent compounds and their microbial products were performed using a Waters/Micromass QqToF-Micro system coupled to a Waters Acquity UPLC system (Micromass, Manchester, UK). Samples from biodegradation experiments were analyzed on a Waters Acquity BEH C18 column (10 mm × 2.1 mm, 1.7 μm particle size). After elution from the column, glibenclamide and atenolol were analyzed in positive ion (PI) mode with a mobile phase consisting of (A) 5 mM aqueous NH$_4$Ac/acetic acid (pH 4.8) and (B) acetonitrile–methanol (2:1, v/v) at 400 μL/min. The elution started at 5% B for 1 min and then it was linearly increased to 60% of B in 8 min, further increased to 95% of B in the next 2 min, and then returned to initial conditions. Total run time, including the conditioning of the column to the initial conditions was 14 min. The injection volume of the sample was 10 μL.

The mass spectrometry analysis on the QqTOF instrument was performed in wide pass quadrupole mode, for MS experiments, with the TOF data being collected between m/z 80 and m/z 800. The capillary and cone voltages were set to 3000 V and 30 V, respectively. Data were collected in the centroid mode, with a scan accumulation time of 1 s. The instrument was operated at a resolution of 5000 (FWHM). The nebulisation gas was set to 500 L/h at a temperature of 350 °C, the cone gas was set to 50 L/h, and the source temperature to 120 °C. All analyses were acquired using an independent reference spray via the LockSpray interference to ensure accuracy and reproducibility. Valine–tyrosine–valine was used as the internal lock mass in the PI mode with [M+H]$^+$ = m/z 380.2185. The LockSpray frequency was set at 11 s. Fragmentation of precursor ions was done by applying collision energies in the range of 10–50 eV, using argon as a collision gas at a pressure of ∼20 psi.

Elemental compositions of the molecular ions and their fragments were determined and exact masses were calculated with the help of MassLynx V4.1 software incorporated in the instrument. Since the software calculation of the accurate mass of cation is performed by adding a hydrogen atom instead of proton, mass of one electron (i.e., 0.0005) was subtracted from the calculated mass [24].

2.4. HPLC/ESI-QqLIT-MS analysis

Further confirmation of the structure of encountered degradation products was carried out on an Agilent Series 1100 liquid chromatograph coupled to an API 4000 QTRAP mass spectrometer (Applied Biosystems/MSD Sciex, Foster City, CA, USA). Due to the fact that the sensitivity of the employed QqTOF instrument was not high enough for the identification of the target compounds at low ng/L concentration level, the API 4000 QTRAP mass spectrometer (Applied Biosystems/MSD Sciex) coupled to a Waters XBridge C18 column was employed. Operated in MRM mode, this instrument enabled the detection of atenolol and a product of its microbial degradation in real wastewater samples.

The chromatographic separations were achieved on a Waters XBridge C18 (100 mm × 2.1 mm, 3.5 μm particle size) equipped with a 10 mm × 2.1 mm guard column of the same packing material. The mobile phases were the same as the one used in the UPLC analysis, whereas the flow rate was 200 μL/min. The gradient was as follows: after 3 min of 85% of aqueous phase (A), the percentage of A was linearly decreased to 5% within 22 min. For the next 7 min elution was performed at 5% of A, and then returning to initial conditions was started. Total run time including the conditioning of the column to the initial conditions was 50 min. The injection volume

was 10 μL. The turbo Ion Spray source was operated in positive ion mode using the following settings for the ion source and mass spectrometer: curtain gas 30 psi, spraying gas 50 psi, drying gas 50 psi, drying gas temperature of 500 °C and ion spray voltage of 4500 V. The declustering potential was 90 V, excitation energy was set to 60 V, and the collision energy was optimized for each compound.

3. Results and discussion

In order to detect possible biodegradation products of the selected pharmaceuticals, samples from batch reactors were analyzed in a full-scan mode at QqTOF-MS instrument. Structural elucidation and interpretation of the fragmentation pathways of the detected metabolites and their parent compounds was facilitated by collision-induced dissociation tandem mass spectrometry (CID-MS/MS). Tables 1 and 2 summarize the exact masses of molecular ions and fragment ions, together with recalculated mass errors and double bond equivalents (DBEs) given by the software. The data presented in Tables 1 and 2 were obtained under optimized conditions of collision energy and cone voltage of the QqTOF mass spectrometer.

3.1. Biodegradation experiments of atenolol

Possible ways for attenuation of β-blocker atenolol in the environment are biodegradation, photolysis and sorption to suspended solids. Considering low values of Henry coefficient (K_H) of atenolol [25], stripped fraction removed by volatilization can be neglected [26]. Literature data on the removal of atenolol in WWTPs is still very scarce and inconsistent; reported removal rates of atenolol vary from 0% to 79% [8,17–21]. This can possibly be explained by the dependency on the operating parameters of the WWTP; the percentage of elimination of atenolol is expected to increase with higher hydraulic retention times (HRTs) applied [20,21]. Biodegradation has been proposed to be the primary mechanism for the removal of this hydrophilic drug in WWTPs [20,27].

During 10 days of sorption experiment no attenuation of the initial concentration of the parent compound was noted, which indicated negligible partitioning of atenolol onto sewage sludge (data not shown). This is in accordance with previously found sorption coefficient (K_D) of atenolol, which was determined to be 0.04 L/g COD [20]. Also, from the estimated log K_{OW} value of atenolol (−0.03) [25], low extent of sorption was to be expected. The partitioning of atenolol in environmental matrices is still questionable, and results of some previous studies pointed out the affinity of atenolol for sediments and suspended solids [19,28]. However, in the experiments conducted in this study possible elimination of atenolol from the liquid phase through sorption processes was excluded, since the experiment settings for sorption and biodegradation were identical and no attenuation of the initial amount of atenolol was seen in the control reactor with autoclaved sludge (data not shown).

The plots of the normalized peak area for atenolol and its biodegradation product vs. time are depicted in Fig. 1, for the three biodegradation trials performed. Since there was no pure standard available for the unknown metabolite of atenolol, only its qualitative determination could be performed. The biodegradation curves represent approximate profiles of the disappearance of the parent compound and formation of the biodegradation product. In 10 mg/L aerated batch reactors, atenolol started to dissipate rapidly with no initial lag-phase. After the first 2 days of experiments, the concentration of atenolol already decreased to around 5 mg/L. Although the kinetic profile was not investigated in this study, this would imply a substantially faster degradation than the one reported by

Table 1
Accurate mass measurements of atenolol[a] and atenololic acid[b] as determined by UHPLC/ESI (+)-QqTOF-MS in MS/MS mode.
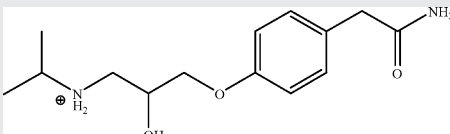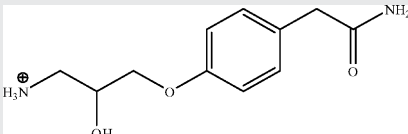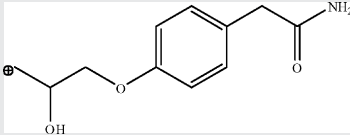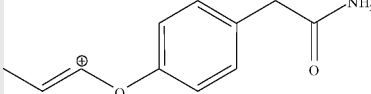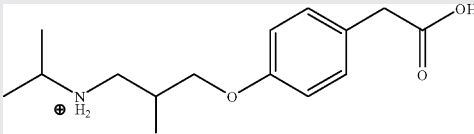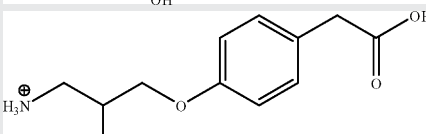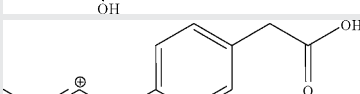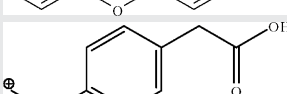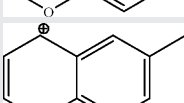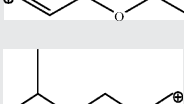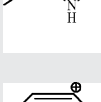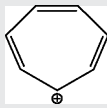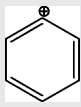
(Fragment) ion	Elemental composition	Structure	Calculated mass (m/z)	Measured mass (m/z)	Relative and absolute error (ppm, mDa)	DBE
Atenolol						
[M+H]$^+$ = 267	[a]$C_{14}H_{23}N_2O_3^+$		267.1704	267.1696	−3.0, −0.8	4.5
m/z = 225	[a]$C_{11}H_{17}N_2O_3^+$		225.1234	225.1222	−5.3, −1.2	4.5
m/z = 208	[a]$C_{11}H_{14}NO_3^+$		208.0969	208.0975	2.9, 0.6	5.5
m/z = 190	[a]$C_{11}H_{12}NO_2^+$		190.0863	190.0874	5.8, 1.1	6.5
Atenololic acid						
[M+H]$^+$ = 268	[b]$C_{14}H_{22}NO_4^+$		268.1544	268.1538	−2.2, −0.6	4.5
m/z = 226	[b]$C_{11}H_{16}NO_4^+$		226.1074	226.0997	−34.0, −7.7	4.5
m/z = 191	[b]$C_{11}H_{11}O_3^+$		191.0703	191.0697	−3.1, −0.6	6.5
m/z = 165	[b]$C_9H_9O_3^+$		165.0547	165.0543	−2.4, −0.4	5.5
m/z = 145	$C_{10}H_9O^+$		145.0648	145.0650[a]; 145.0653[b]	1.4[a], 0.2[a]; 3.4[b], 0.5[b]	6.5
m/z = 133	$C_9H_9O^+$		133.0648	133.0658[a], 133.0642[b]	7.5[a], 1.0[a]; −4.5[b], −0.6[b]	5.5
m/z = 116	$C_6H_{14}NO^+$		116.1070	116.1071[a], 116.1060[b]	0.9[a], 0.1[a]; −8.6[b], −1.0[b]	0.5
m/z = 107	$C_7H_7O^+$		107.0492	107.0496[a], 107.0455[b]	3.7[a], 0.4[a]; −34.6[b], −3.7[b]	4.5

Table 1 (*Continued*).

(Fragment) ion	Elemental composition	Structure	Calculated mass (m/z)	Measured mass (m/z)	Relative and absolute error (ppm, mDa)	DBE
$m/z = 91$	$C_7H_7^+$		91.0543	91.0560[a], 91.0546[b]	18.7[a], 1.7[a]; 3.3[b], 0.3[b]	4.5
$m/z = 77$	$C_6H_5^+$		77.0386	77.0387[a], 77.0398[b]	1.3[a], 0.1[a]; 15.6[b], 1.2[b]	4.5
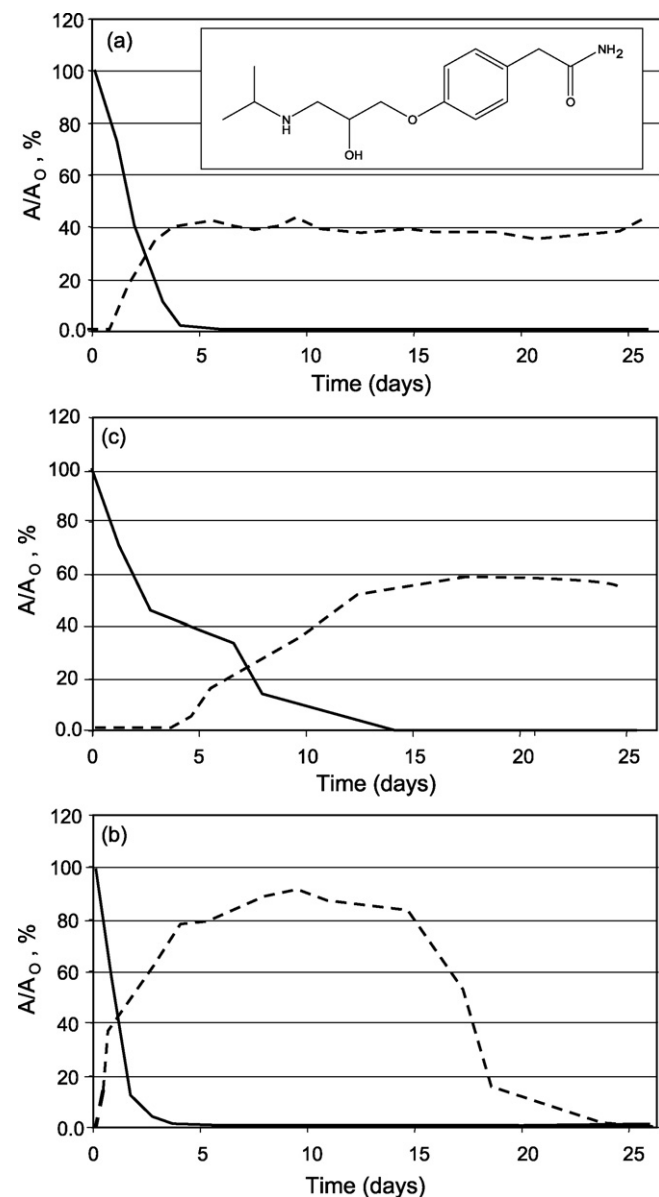
Fig. 1. The peak areas normalized to their initial values (i.e., at $t = 0$) are presented vs. time for atenolol (—) and atenololic acid (– – –) in (a) CAS sludge experiments at 10 mg/L concentration, (b) CAS sludge experiments at 50 μg/L concentration, and (c) MBR sludge experiments at 10 mg/L concentration.

Maurer et al. [20]. Faster dissipation of atenolol in our experiments could be due to the higher initial amount of specific degraders and thus better biodegradation capabilities of the CAS sludge used. Also, volume of sludge used, amount of substrate and total volume of active biomass will influence strongly the biodegradation profile obtained in the experiment [29,30]. After 3 days, 90% of the parent compound had disappeared.

At the same time with the disappearance of the atenolol peak ([M+H]$^+$ 267, retention time, $t_R = 2.97$ min), a new signal was detected at $t_R = 3.09$ min after the first 5 h of the CAS biodegradation test. The intensity of this signal was growing as the atenolol peak was disappearing (Fig. A of the Supporting Information). The ESI (+)-MS/MS experiments performed with the QqTOF-MS instrument showed a very similar spectrum of this peak with the MS/MS spectrum of the parent compound (see Fig. 2). The new compound was determined as a molecular ion, [M+H]$^+$, of m/z: 268, which was assumed to be an outcome of a bacterial hydrolysis of amide bond. Therefore, the substitution of an amine group by a hydroxyl group afforded a product with a chemical name 4-{2-hydroxy-3-[(1-methyl)amino]propoxy}benzeneacetic acid, here denominated atenololic acid. As this signal was not observed in the chromatogram corresponding to the control sample of sterilized sludge it originated from biodegradation of atenolol. Also, the possibility of chemical hydrolysis was excluded since atenololic acid was not detected in the sorption experiment with autoclaved sludge that was at the same pH as sludge in the batch reactors at the beginning of the experiment (i.e., pH 6.3–6.5). Moreover, it was reported that hydrolysis of atenolol into 4-[(3-isopropyloamino)-2-propenoxy]phenylacetic acid required a very acidic environment (pH ≤ 1) [31]. In this process, besides of amide group hydrolysis double bond is also generated through dehydration process in the aliphatic fragment.

The instant decline in atenolol concentration paralleled with the formation of atenololic acid suggested that it was formed as a primary degradation product, i.e., by a direct transformation of the parent compound. The biodegradation product of atenolol reached its maximum concentration on the day 5, which remained unchanged until the end of the biodegradation test (i.e., day 26). In other words, although the parent compound was degraded rapidly, the product of its microbial degradation by microorganisms was more stable and proved to be a biologically recalcitrant compound.

A second experiment with activated sludge spiked at 50 μg/L of atenolol proved that the degradation route was independent on the initial concentration of the compound. However, degradation rate decreased after the first 2 days, with 90% of the parent compound degraded after 10 days (see Fig. 1b), which is three times longer than the time needed at a concentration of 10 mg/L of atenolol. While 50% of the initial amount of atenolol disappeared after approximately 42 h, the rest of atenolol was transformed more slowly.

Table 2

Accurate mass measurements of glibenclamide[a] and glibenclamide hydroxide[b] as determined by UHPLC/ESI (+)-QqTOF-MS in MS/MS mode.
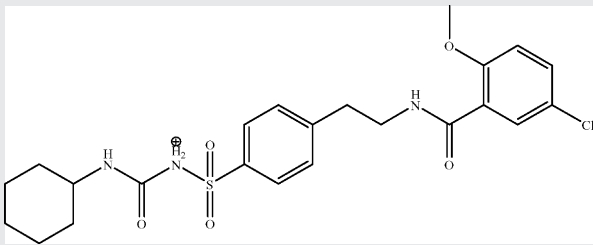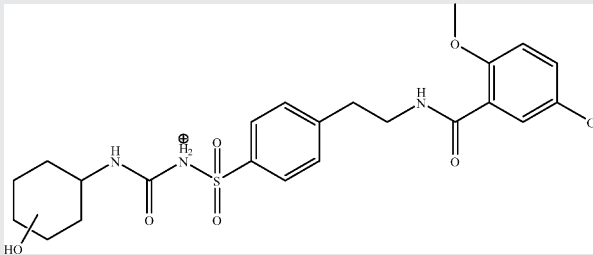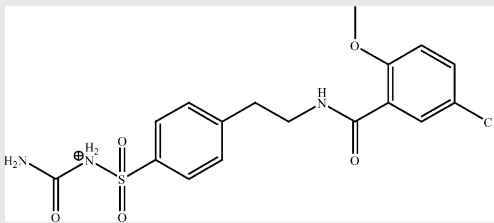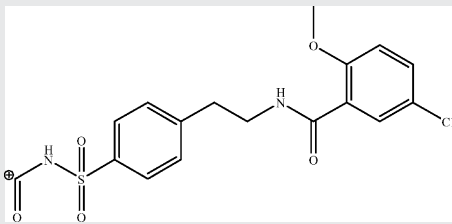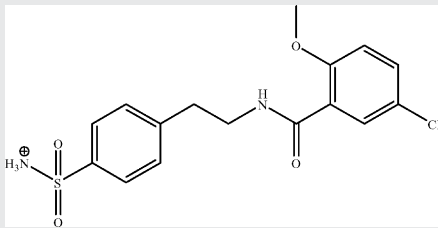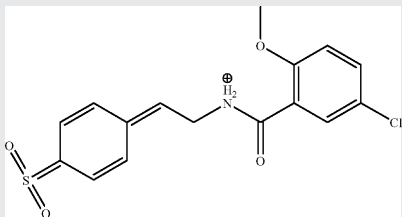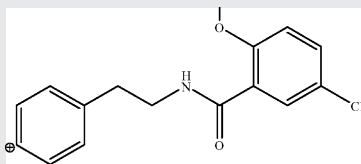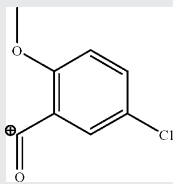
(Fragment) ion	Elemental composition	Structure	Calculated mass (m/z)	Measured mass (m/z)	Relative error (ppm, mDa)	DBE
					Glibenclamide	
[M+H]$^+$ = 494	[a]$C_{23}H_{29}ClN_3O_5S^+$		494.1511	494.1516	1.0, 0.5	10.5
Glibenclamide hydroxide						
[M+H]$^+$ = 510	[b]$C_{23}H_{29}ClN_3O_6S^+$		510.1461	510.1431	−5.9, −3.0	10.5
m/z = 412	$C_{17}H_{19}ClN_3O_5S^+$		412.0729	412.0777[a], 412.0775[b]	11.6[a], 4.8[a]; 11.2[b], 4.6[b]	9.5
m/z = 395	$C_{17}H_{16}ClN_2O_5S^+$		395.0463	395.0452[a], 395.0476[b]	−2.8[a], −1.1[a]; 3.3[b], 1.3[b]	10.5

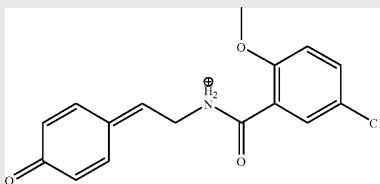J. Radjenović et al. / J. Chromatogr. A 1210 (2008) 142–153

147

Table 2 (*Continued*)

(Fragment) ion	Elemental composition	Structure	Calculated mass (m/z)	Measured mass (m/z)	Relative error (ppm, mDa)	DBE
$m/z = 369$	$C_{16}H_{18}ClN_2O_4S^+$		369.0671	369.0672[a], 369.0676[b]	0.3[a], 0.1[a]; 1.3[b], 0.5[b]	8.5
$m/z = 352$	$C_{16}H_{15}ClNO_4S^+$		352.0405	352.0440[a], 352.0432[b]	9.9[a], 3.5[a]; 7.7[b], 2.7[b]	9.5
$m/z = 304$	$C_{16}H_{15}ClNO_3^+$		304.0735	304.0750[a], 304.0748[b]	4.9[a], 1.5[a]; 4.3[b], 1.3[b]	9.5
$m/z = 288$	$C_{16}H_{15}ClNO_2^+$		288.0786	288.0803[a], 288.0812[b]	5.9[a], 1.7[a]; 9.0[b], 2.6[b]	9.5
$m/z = 169$	$C_8H_6ClO_2^+$		169.0051	169.0056[a], 169.0057[b]	3.0[a], 0.5[a]; 3.5[b], 0.6[b]	5.5
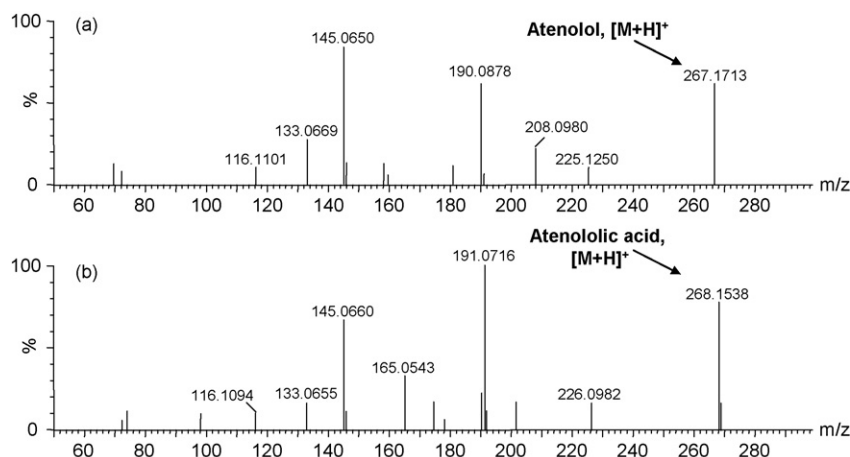
Fig. 2. Spectra of atenolol and atenololic acid from ESI (+)-MS/MS experiments with a QqTOF instrument whereas the cone voltages 25 V and collision energies were 20 eV and 17 eV for atenolol and atenololic acid, respectively. (a) Standard mixture of atenolol in methanol/water (v/v, 25/75) at 10 mg/L; (b) CAS batch reactor sample (10 mg/L) taken at t = 3.2 days.

The SS concentration of MBR sludge was 20 g/L, which was significantly higher compared to the one measured for CAS sludge (i.e., 4 g/L). This was a consequence of a very long SRT (i.e., 3 months) applied in a laboratory-scale MBR. Prolonged SRT should imply better adaptation of sludge to the present micropollutants. Moreover, in a previous study [8], atenolol was encountered at high concentrations (in μg/L) in the primary effluent, i.e., influent to the MBR and CAS treatments. While practically no elimination of atenolol was found in CAS (i.e., <20% removal), in the MBR it was attenuated from the primary effluent with around 65.5% efficiency [8]. Therefore, it was expected that MBR sludge would have better biodegradation capabilities towards this micropollutant.

Indeed, atenolol dissipated faster than in batch reactors with conventional sludge, with 90% of the parent compound disappearing after the first 2 days (see Fig. 1c). Surprisingly high amount of the formed atenololic acid was seen after day 3 (i.e., around 80% of the initial intensity of atenolol peak), whereas in CAS experiments it reached only around 40% of the initial amount of the parent compound. This can be considered as another consequence of enhanced microbial activity of MBR sludge, together with higher concentration of SS and more diverse microorganisms present. Moreover, while this metabolite was not degraded by CAS sludge, in MBR batch reactors its concentration started to decrease after 15 days of the experiment, as it can be seen from Fig. 3c. Thus, the ultimate biodegradability of atenolol in MBR sludge was substantially higher than in the conventional one. This suggested that a diverse biocenosis is developed, characteristic for an MBR, with great biodegrading capacity for the polar, hydrophilic pharmaceutical atenolol and its degradation product, atenololic acid. Although very long SRT of MBR sludge would permit proliferation of nitrifying bacteria, their role can be ruled out here since the optimum pH for their growth is between pH 7.5 and 8.6, whereas in the batch reactors it was dropped from pH 6.3 to 5.1 by day 5.

3.2. Identification of biodegradation products: fragmentation pathways of atenolol and atenololic acid

In Table 1 are presented calculated and measured masses of fragment ions of atenolol and atenololic acid, determined by ESI (+)-MS/MS experiments on the QqTOF-MS instrument. Since all fragment ions had an even number of electrons (i.e., DBE was half integer number in all cases), all neutral losses had likewise even electron configurations [32]. The most abundant fragments detected in the MS^2 spectrum of atenolol by QqTOF-MS were m/z

190 and m/z 145 (see Fig. 2). Their formation pathways were elucidated in MS^3 experiments performed by QqLIT-MS (see Fig. 3).

Two separate fragmentation pathways were elucidated by QqLIT-MS. The neutral loss of water from the protonated molecules at m/z 267 and 268 generated the fragment ions m/z 249 and m/z 250, respectively, which could not be detected in the MS^2 spectra of the QqTOF-MS. The subsequent losses of isopropylamine (59 Da) resulted in m/z 190 and m/z 191 fragment ions, observed also in the spectra obtained by QqTOF-MS for atenolol and atenololic acid, respectively. Then, loss of ammonia from m/z 249 yielded the m/z 232 ion in the QqLIT mass spectrum of atenolol, whereas m/z 250 ion in the spectrum of atenololic acid did not fragment in the same way.

On the other side, after loss of propene molecule (42 Da) from the molecular ions m/z 267 and m/z 268, fragment ions m/z 225 and m/z 226 were formed, respectively. Next, subsequent losses of ammonia and water from the fragment ion at m/z 225 yielded ions with m/z 208 and m/z 190, respectively. This loss of 77 Da (i.e., isopropylamine and water) had also been previously reported for β-blockers bearing the –NH–CH(CH$_3$)$_2$ side chain, under CID conditions in a triple quadrupole (QqQ) instrument [18]. However, fragment ion m/z 226 originating in the spectrum of atenololic acid broke up directly into m/z 191 (loss of ammonia and water).

The m/z 173 fragment ion was further generated from m/z 190 by losing an ammonia molecule from the amide group. Similar to the previously mentioned fragment ions at m/z 249, m/z 250 and m/z 232, m/z 173 ion was not observed in the MS^2 experiment on the QqTOF-MS system. After cleavage of a CO molecule and intramolecular cyclization and rearrangement, m/z 145 fragment ion was formed. However, this succession (i.e., m/z 191 → m/z 173 → m/z 145) was not observed in the spectrum of atenololic acid, where only m/z 145 fragment ion was detected. The ion m/z 145 was detected as a very strong signal, whereas it was also previously observed in the MRM analysis of atenolol by QqQ [33].

The following fragment ions were detected in the spectra of both atenolol and atenololic acid. The m/z 116 ion originating from molecular ions, [M+H]$^+$, of m/z 267 and 268 represented losses of p-hydroxyphenylacetamide and p-hydroxyphenylacetic acid, respectively. On the other side, possibly the elimination of acetamide (58 Da) and acetic acid (59 Da) moiety from m/z 190 and m/z 191, respectively, afforded an ion m/z 133. The phenyl and benzylium ions were detected as well (m/z 77 and m/z 91, respectively), whereas the last one is stabilized over tropylium cation. Finally, m/z 107 ion was observed, though with a very low intensity in
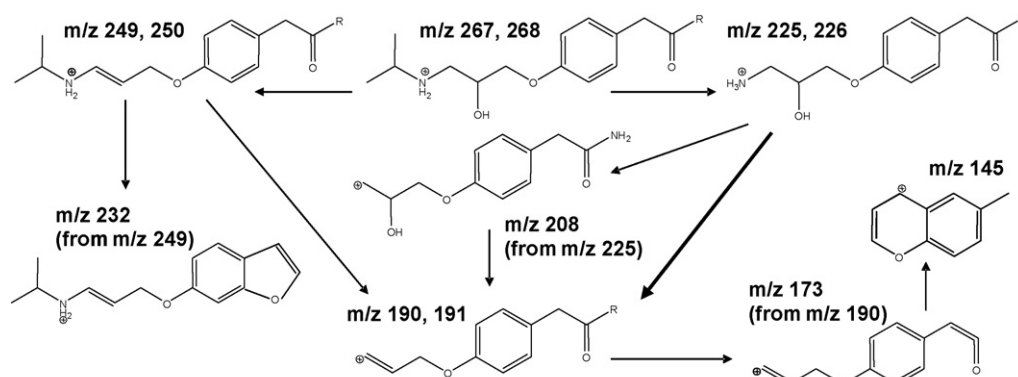
Fig. 3. Proposed fragmentation pathway of atenolol ($R = NH_2$) and atenololic acid ($R = OH$) under ESI (+) conditions as derived from MS^2 and MS^3 experiments in the QqLIT mass spectrometer. In the structures containing the residue R, the first m/z value corresponds to the ion derived from atenolol, and the second one to the atenololic acid.

the case of atenololic acid (see Table 1). Due to their low intensity, fragmentation pathways could not be established for these ions by QqLIT-MS.

3.3. Biodegradation experiments of glibenclamide

The sorption experiments showed no removal of glibenclamide by sorbing to sludge particles, since its concentration in the test flask with autoclaved sludge remained unchanged during 10 days.

As far as biodegradability is concerned, the decay rate of glibenclamide was substantially lower than the one seen for atenolol. The plots of the normalized peak area for glibenclamide and its metabolite vs. time are depicted in Fig. 4, for the three biodegradation tests performed. Like in the case of atenolol, the plots presented are estimations of the degradation profile of glibenclamide and the formation profile of its metabolite, due to the lack of analytical standard for the unknown compound.

On the 10th day, the maximum amount of metabolite is formed (i.e., around 30% of the initial intensity of glibenclamide peak) that remains fairly constant until the end of the experiment (see Fig. 4a). Similar to atenololic acid, more polar, hydroxylated metabolite of glibenclamide also displayed higher resistance to biodegradation by the biocenosis of sewage sludge. The degradation of 90% of the parent compound was completed after approximately 5.5 days. Moreover, pseudo lag-phase of around 3 days was seen (see Fig. 4a), which indicated that microorganisms capable of metabolizing glibenclamide needed to proliferate first. When this experiment was repeated with the same type of sampled sludge and at the same spiked concentration of glibenclamide, the duration of lag-phase was similar although further degradation was slightly slower, with 90% of the parent compound disappearing after approximately 6 days (data not shown).

On the other side, full-scan experiments performed by UHPLC–QqTOF-MS instrument showed the appearance of new peak after the first 20 h, at a retention time of 7.3 min (see Figure B of the Supporting Information). This microbial metabolite had a molecular ion [M+H]$^+$ of m/z 510, which was assumed to be the outcome of bacterial hydroxylation of glibenclamide. The MS/MS spectrum of this hydroxylated metabolite is illustrated at Fig. 5.

In 50 μg/L batch reactors, however, no lag-phase was noted, but the degradation rate of glibenclamide was substantially slower leaving 10% of the compound after 10 days of the experiment (see Fig. 4b). Similar to the case of atenolol, at lower substrate concentrations microorganisms were less efficient in its metabolization. Parallel to the disappearance of the parent compound, gliben-

clamide hydroxide was formed after the first 5 days. The maximum amount of glibenclamide hydroxide formed comprised only around 10% of the initial amount of the parent compound, and it did not dissipate any further.
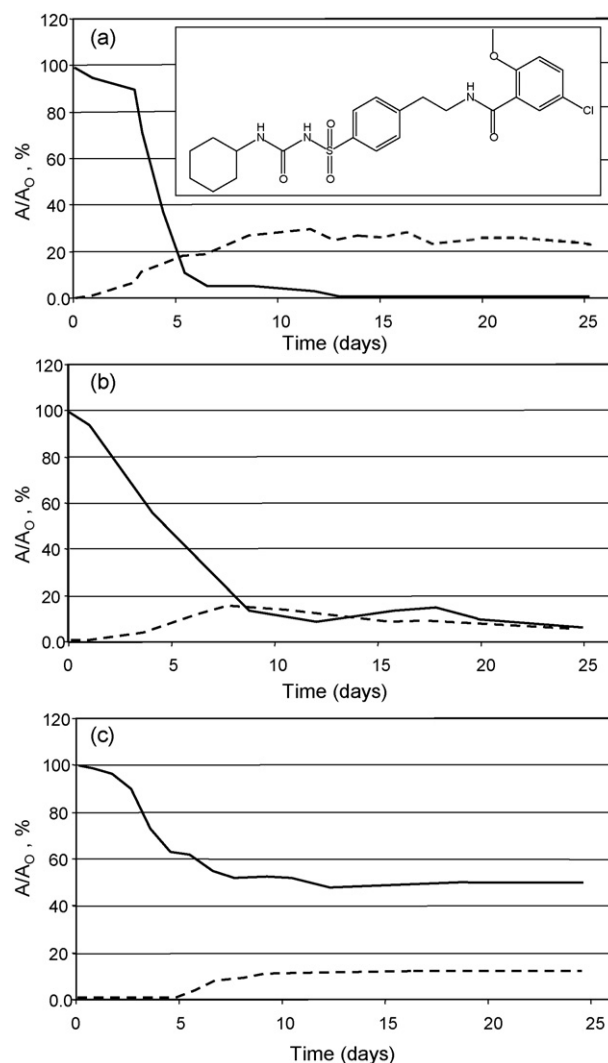
Fig. 4. The peak areas normalized to their initial values (i.e., at $t = 0$) are presented vs. time for glibenclamide (—) and glibenclamide hydroxide (– – –) in (a) CAS sludge experiments at 10 mg/L concentration, (b) CAS sludge experiments at 50 μg/L concentration, and (c) MBR sludge experiments at 10 mg/L concentration.
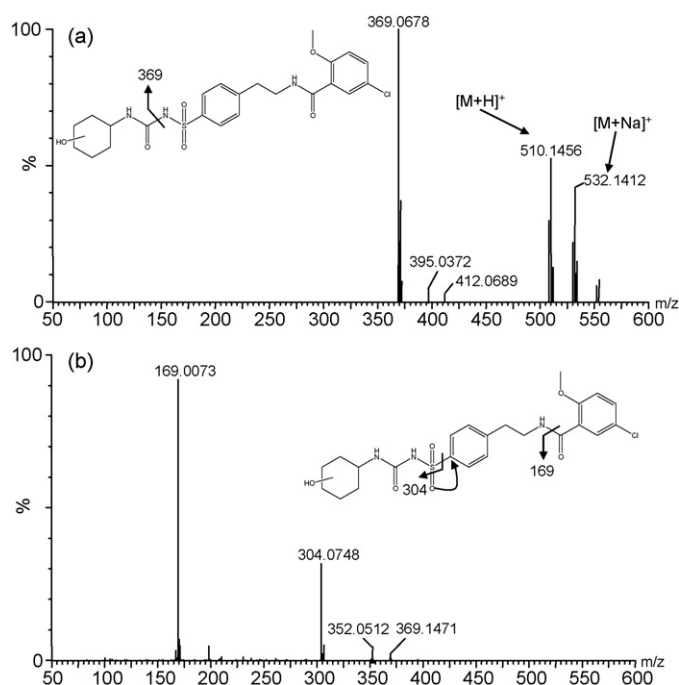
Fig. 5. Spectra of glibenclamide hydroxide (*m/z* 510.146) obtained with the QqTOF instrument for the sample taken after 6 days from CAS batch reactor (10 mg/L), in (a) ESI (+)-MS full-scan mode, and (b) ESI (+)-MS/MS experiments at collision energy of 30 eV.

In a previous study conducted at WWTP Rubí [8] only 45% removal of glibenclamide during CAS treatment was observed, whereas a laboratory-scale MBR did not show any enhancement in its elimination in contrast to other pharmaceutical residues investigated (i.e., 47% removal of glibenclamide). In batch experiments with MBR sludge glibenclamide was degraded only with around 50% efficiency. The metabolite glibenclamide hydroxide was spotted on the day 5, reaching approximately 10% of the initial amount of glibenclamide. However, the MBR sludge did not degrade this microbial metabolite any further (see Fig. 4c). It could be that the adaptation of microbial community was interrupted, due to the fact that a number of factors may interfere with their acclimation. The influence of temperature or pH on the adaptation of microorganisms was ruled out since these factors did not have strange variations whatsoever. The observed deterioration in biodegradation by MBR sludge could be explained by insufficient aeration of

a batch reactor. Since the SS concentration in MBR experiment was significantly higher than for the conventional sludge, it could be that the microbial hydroxylation pathway was obstructed due to the lack of oxygen in the reactor. Also, growth and metabolism of microbial population may be subjected to subtle changes in their environment. The consequences of microbial succession (i.e., selection and development of sequential microbial populations) are changes such as decrease in available nutrients, alterations in pH or redox potential, disappearance of oxygen, to name just a few. Thus, initial microbial population may become self-limiting and growth of other microorganisms can be favoured, which emerge as a new dominant population.

3.4. Identification of biodegradation products: fragmentation pathways of glibenclamide and glibenclamide hydroxide

As it can be seen from Fig. 6, proposed fragmentation pathways are identical for glibenclamide and glibenclamide hydroxide. The most abundant fragment ion in ESI (+)-MS/MS experiments for both the parent compound and its hydroxylated metabolite was ion *m/z* 369, formed by the cleavage of cyclohexylamide moiety ($C_6H_5N \cdot HCO$). This kind of fragmentation of glibenclamide–hydroxide left two possibilities for the hydroxyl group to attach: either on the cyclohexyl ring or on the side chain nitrogen atom. However, the presence of the fragment ion *m/z* 412 in the spectrum obtained on the QqTOF-MS indicated that hydroxylation had taken place on a cyclohexyl ring, since this ion was formed by the separation of cyclohexyl and hydroxycyclohexyl moiety from molecular ions *m/z* 494 and *m/z* 510, respectively. Most probably it was attached at the 3 or 4 positions, thus giving 4-hydroxy and/or 3-hydroxy derivative of glibenclamide, similar to the human metabolism of this drug [15]. The exact position of the hydroxyl group, however, could not be determined neither by MS/MS experiments at the QqTOF instrument. In Table 2 accurate mass measurements and DBE values are summarized for molecular and fragment ions of glibenclamide and glibenclamide hydroxide.

The cleavage of the terminal amide bond attached to the cyclohexyl ring yielded an ion at *m/z* 395. Both *m/z* 369 and 395 fragment ions were precursors for *m/z* 169 ion in QqLIT-MS, form by the cleavage of amide bond (see Fig. 6). This ion could not be broken down into any detectable fragment ions, probably due to its high stability. The origin of other fragment ions observed in ESI (+)-MS/MS experiments on the QqTOF-MS system could not be determined by QqLIT-MS. Nevertheless, most probably a cleavage of a sulphonamide bond in *m/z* 369 resulted in *m/z* 352 fragment
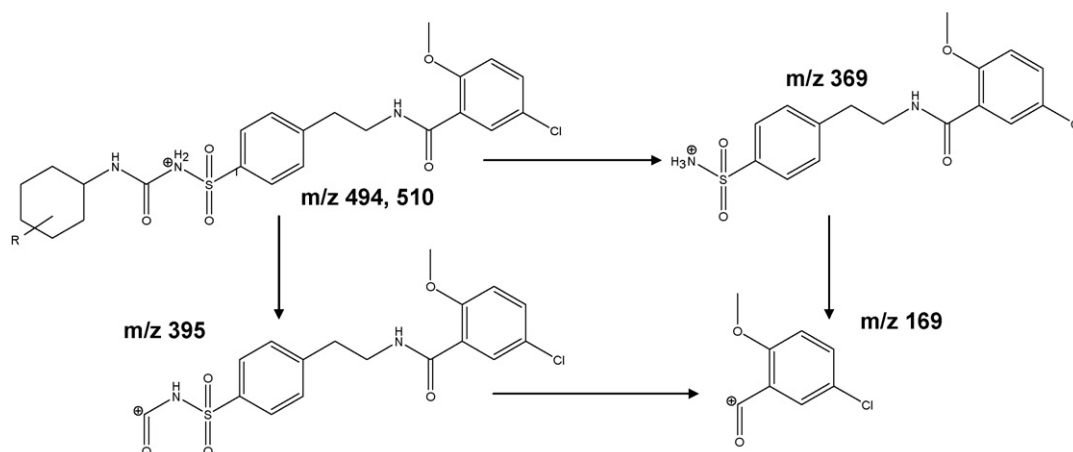
Fig. 6. Proposed fragmentation pathway of glibenclamide (R = H) and glibenclamide hydroxide (R = OH) under ESI (+) conditions as derived from MS^2 and MS^3 experiments in the QqLIT mass spectrometer.
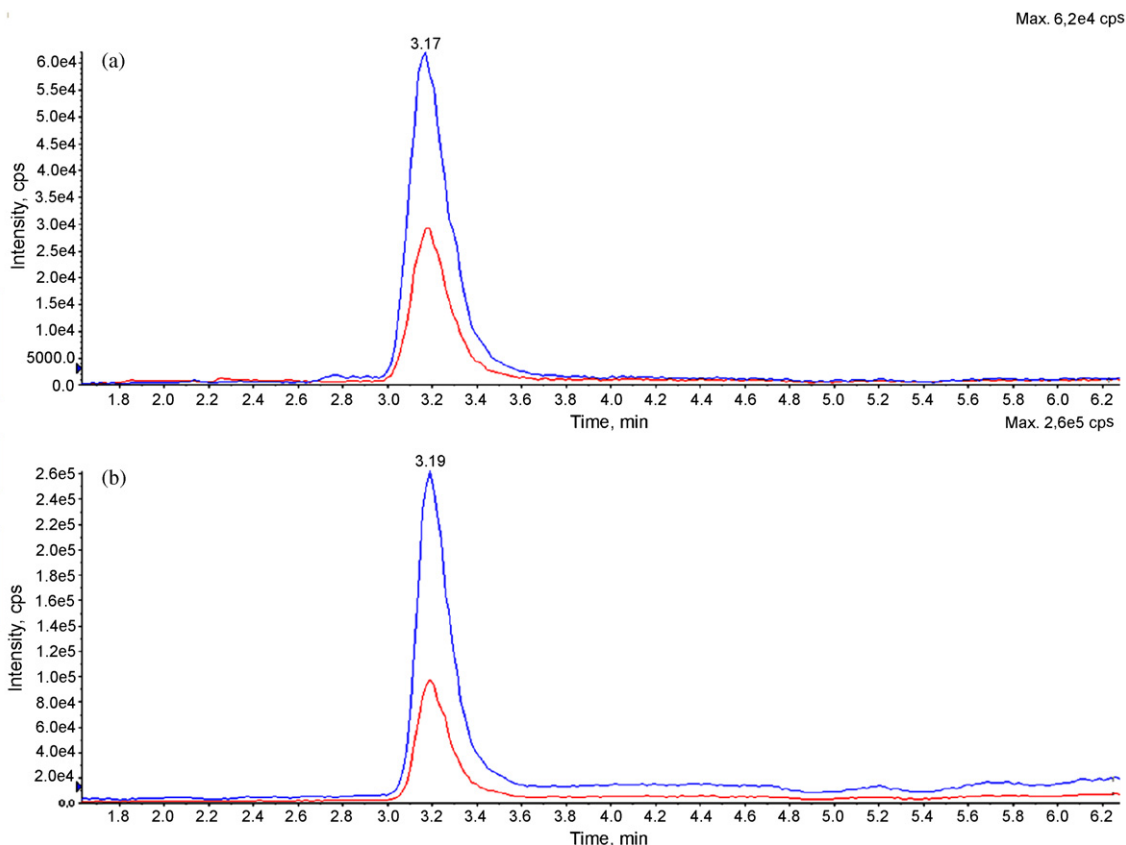
Fig. 7. Extracted ion chromatograms (XIC) of MRM chromatogram of CAS effluent sample from WWTP Terrassa, showing the two transitions for (a) atenololic acid (m/z 268.0 → m/z 145.0, m/z 268.0 → m/z 191.0) and (b) atenolol (m/z 267.0 → m/z 145.0, m/z 267.0 → m/z 190.0).

ion, that was a precursor for a low intensity m/z 304 fragment ion (i.e., loss of SO from SO$_2$ group). Apparently a cleavage of S–C bond at the benzene ring and loss of sulphur dioxide generated an ion at m/z 288.

3.5. Detection of atenolol and atenololic acid in real wastewater samples

HPLC–ESI (+)-QqLIT-MS analysis enabled confirmation of the presence of atenolol and its biodegradation product in real wastewater samples. Out of six composite samples of the primary effluent (i.e., influent of CAS treatment) and secondary effluent (i.e., effluent of CAS treatment) taken at WWTP Rubí, atenolol was detected in all primary effluent samples at 3.1–2.2 µg/L concentration, whereas its concentration in the secondary effluents was lower (i.e., 0.62–1.3 µg/L). On the other side, atenololic acid was detected in only one (out of three) primary effluent sample with a very low intensity signal, whereas its peak area in all three secondary effluents was significantly higher. Fig. 7 illustrates the chromatograms of one of the CAS effluent samples analyzed, recorded in the ESI (+)-MRM mode. The quantitative analysis of atenololic acid was not possible, due to the absence of pure analytical standard for this newly identified compound.

The concentration of glibenclamide in the primary effluent samples was in the range of 0.57–1.2 µg/L. Although the concentration levels detected for the effluent of CAS treatment were lower (i.e., 0.12–0.4 µg/L) thus indicating possible (bio)transformation/degradation of glibenclamide during the treatment, the microbial metabolite identified in biodegradation experiments, glibenclamide hydroxide, was not detected in any of the wastewater samples taken at WWTP Rubí.

4. Conclusions

The biodegradation pathways of atenolol and glibenclamide were identical when degraded by MBR and CAS sludge. In the case of atenolol, bacterial hydrolysis of amide bond led to the same primary biodegradation product, atenololic acid. However, ultimate biodegradability of this β-blocker was higher in MBR sludge, since not only the parent compound but also its microbial metabolite were completely degraded after 2 days and 20 days. However, hydroxylated metabolite of glibenclamide turned out to be a persistent product in both experiments. Moreover, deterioration in the removal of both glibenclamide and glibenclamide hydroxide was observed in a test flask with MBR sludge. The product of microbial degradation of atenolol (i.e., atenololic acid) obtained in laboratory experiment was detected in real wastewater effluent samples at concentration levels equal to the one of the parent compound. On the other side, the occurrence study for glibenclamide hydroxide did not give any positive results, although glibenclamide was present in the primary effluent in WWTP Rubí.

The study has implications for better understanding of environmental fate of the two pharmaceuticals investigated. The newly detected metabolites atenololic acid and glibenclamide hydroxide could be more persistent and present in concentrations even higher than the parent compound, thus they should be included in environmental studies of atenolol and glibenclamide. The main impediment to the encompassment of biodegradation and/or biotransformation products into the multi-residue methods is the lack of commercially available analytical standards, which would enable their confirmation in the environmental samples. Our future work will be focused on the synthesis of atenololic acid and gliben-

clamide hydroxide, and their quantitative determination in the aquatic environment. Also, ecotoxicological studies of the parent compounds and their microbial products will be performed in order to evaluate the effect that these pharmaceutical residues might have in the environment.

Acknowledgments

Appendix A. Supplementary data

Supplementary data associated with this article can be found, in the online version, at doi:10.1016/j.chroma.2008.09.060.

References

[1] L.J. Schulman, E.V. Sargent, B.D. Naumann, E.C. Faria, D.G. Dolan, J.P. Wargo, Hum. Ecol. Risk Assess. 8 (2002) 657.
[2] C. Zwiener, S. Seeger, T. Glauner, F.H. Frimmel, Anal. Bioanal. Chem. 372 (2002) 569.
[3] P. Eichhorn, P.L. Ferguson, S. Pérez, D.S. Aga, Anal. Chem. 77 (2005) 4176.
[4] J.B. Quintana, S. Weiss, T. Reemtsma, Water Res. 39 (2005) 2654.
[5] S. Pérez, P. Eichhorn, M.D. Celiz, D.S. Aga, Anal. Chem. 78 (2006) 1866.
[6] S. Pérez, P. Eichhorn, D.S. Aga, Environ. Toxicol. Chem. 24 (2005) 1361.
[7] J. Radjenović, M. Matošić, I. Mijatović, M. Petrovic, D. Barceló, in: D. Barceló, M. Petrović (Eds.), Membrane bioreactor (MBR) as advanced wastewater treatment technology. Emerging Contaminants from Industrial and Municipal Wastewaters, Springer-Verlag Berlin and Heidelberg Gmbh & Co. K, 2008.
[8] J. Radjenović, M. Petrovic, D. Barceló, Anal. Bioanal. Chem. 387 (2007) 1365.
[9] M. Clara, B. Strenn, N. Kreuzinger, H. Kroiss, O. Gans, E. Martinez, Water Res. 39 (2005) 4797.
[10] K. Kimura, H. Hara, Y. Watanabe, Environ. Sci. Technol. 41 (2007) 3708.
[11] B. Lesjean, R. Gnirrs, H. Buisson, S. Keller, A. Tazi-Pain, F. Luck, Water Sci. Technol. 52 (2005) 453.
[12] K. Kimura, H. Hara, Y. Watanabe, Desalination 178 (2005) 135.
[13] C. Dollery (Ed.), Therapeutic Drugs, Churchill Livingstone, Edinburgh, 1991.
[14] B.I. Escher, N. Bramaz, M. Richter, J. Lienert, Environ. Sci. Technol. 40 (2006) 7402.
[15] L. Balant, J. Fabre, G.R. Zahnd, Eur. J. Clin. Pharmacol. 8 (1975) 63.
[16] L. Lishman, S.A. Smyth, K. Sarafin, S. Kleywegt, J. Toito, T. Peart, B. Lee, M. Servos, M. Beland, P. Seto, Sci. Total Environ. 367 (2006) 544.
[17] N. Paxeus, Water Sci. Technol. 50 (2004) 253.
[18] H.B. Lee, K. Sarafin, T.E. Peart, J. Chromatogr. A 1148 (2007) 158.
[19] S. Castiglioni, R. Bagnati, R. Fanelli, F. Pomati, D. Calamari, E. Zuccato, Environ. Sci. Technol. 40 (2006) 357.
[20] M. Maurer, B.I. Escher, P. Richle, C. Schaffner, A.C. Alder, Water Res. 41 (2007) 1614.
[21] M. Gros, M. Petrovic, D. Barceló, Environ. Toxicol. Chem. 26 (2007) 1553.
[22] A. Carucci, G. Cappai, M. Piredda, J. Environ. Sci. Health A Tox. Hazard. Subst. Environ. Eng. 41 (2006) 1831.
[23] M. Cleuvers, Chemosphere 59 (2005) 199.
[24] I. Ferrer, E.M. Thurman, Rapid Commun. Mass Spectrom. 21 (2007) 2538.
[25] http://www.syrres.com/.
[26] A. Joss, S. Zabczynski, A. Göbel, B. Hoffmann, D. Löffler, C.S. McArdell, T.A. Ternes, A. Thomsen, H. Siegrist, Water Res. 40 (2006) 1686.
[27] L.N. Nikolai, E.L. McClure, S.L. MacLeod, C.S. Wong, J. Chromatogr. A 1131 (2006) 103.
[28] D. Calamari, E. Zuccato, S. Castiglioni, R. Bagnati, R. Fanelli, Environ. Sci. Technol. 37 (2003) 1241.
[29] F. Ingerslev, L. Torang, N. Nyholm, Environ. Toxicol. Chem. 19 (2000) 2443.
[30] B. Clark, J.G. Henry, D. Mackay, Environ. Sci. Technol. 29 (1995) 1488.
[31] J. Krzek, A. Kwiecien, M. Zylewski, Pharm. Dev. Technol. 11 (2006) 409.
[32] F. McLafferty (Ed.), Interpretation of Mass Spectra, University Science Books, Mill Valley, CA, 1980.
[33] M.D. Hernando, M. Petrović, A.R. Fernández-Alba, D. Barceló, J. Chromatogr. A 1046 (2004) 133.